

MMSE-Based CFO Compensation for Uplink OFDMA Systems with Conjugate Gradient

Kilbom Lee, *Student Member, IEEE*, Sang-Rim Lee, *Student Member, IEEE*,
Sung-Hyun Moon, *Member, IEEE*, and Inkyu Lee, *Senior Member, IEEE*

Abstract—In this paper, we present a low-complexity carrier frequency offset (CFO) compensation algorithm based on the minimum mean square error (MMSE) criterion for uplink orthogonal frequency division multiple access systems. CFO compensation with an MMSE filter generally requires an inverse operation on an interference matrix whose size equals the number of subcarriers. Thus, the computational complexity becomes prohibitively high when the number of subcarriers is large. To reduce the complexity, we employ the conjugate gradient (CG) method which iteratively finds the MMSE solution without the inverse operation. To demonstrate the efficacy of the CG method for our problem, we analyze the interference matrix and present several observations which provide insight on the iteration number required for convergence. The analysis indicates that for an interleaved carrier assignment scheme, the maximum iteration number for computing an exact solution is at most the same as the number of users. Moreover, for a general carrier assignment scheme, we show that the CG method can find a solution with far fewer iterations than the number of subcarriers. In addition, we propose a preconditioning technique which speeds up the convergence of the CG method at the expense of slightly increased complexity for each iteration. As a result, we show that the CFO can be compensated with substantially reduced computational complexity by applying the CG method.

Index Terms—CFO, compensation, OFDMA, conjugate gradient.

I. INTRODUCTION

ORTHOGONAL frequency division multiplexing access (OFDMA) is a popular multi-carrier transmission scheme that enables multiple users to transmit parallel data streams at a high data rate [1] [2]. OFDMA achieves high spectral efficiency in a multiuser environment by dividing the total available band-width into narrow orthogonal subbands. The divided subbands are allocated to mobile users (MUs) according to carrier assignment schemes such as a subband-based carrier assignment scheme (SCAS), an interleaved CAS (ICAS) and a generalized CAS (GCAS) [3]. However, the OFDMA is sensitive to carrier frequency offset (CFO) caused

by a Doppler shift or mismatch between the frequencies of the transmitter and the receiver oscillators [4]. The CFO destroys orthogonality among the subcarriers and leads to inter-carrier interference and multi access interference (MAI) in uplink OFDMA systems, which cause unacceptable bit error rate (BER) performance [5]. Thus, CFO compensation is important for reliable detection of transmitted data.

CFO compensation by the minimum mean square error (MMSE) filter is generally simple and efficient. However, this method requires the inversion of a matrix whose size equals the number of subcarriers. To circumvent the complexity issue, the authors in [6] suggested a low-complexity MMSE receiver (LMMSE) based on the approximate banded matrix. In contrast, interference cancellation (IC) schemes such as those in [7]–[9] mitigate the MAI by reconstructing and removing the interfering signals in the frequency domain and iteratively detect the transmitted data. However, these IC schemes exhibit a performance loss and slow convergence as the CFOs increase. The authors in [10] recently proposed a subcarrier-grouped MMSE based IC scheme (SCG-MMSE) which performs hard symbol detection for each IC unit, and it shows better performance and faster convergence even for large CFOs.

In this paper, we employ the conjugate gradient (CG) method to compute the MMSE filter output without an inverse operation. The CG is an iterative method for linear equations which have a positive definite matrix; it is particularly suitable for a large sparse matrix [11]. In our work, we show that the CG method can quickly find the solution to our problem by using the fact that its convergence depends strongly on the eigenvalue distribution of the matrix [12].

Our main contribution in this paper is to demonstrate the efficacy of the CG-based MMSE filter. For the ICAS, we prove that the covariance matrix of the MMSE filter is Hermitian block-circulant and that the number of distinct eigenvalues is at most the number of MUs. Moreover, for the GCAS, we derive an upper bound of the maximum eigenvalue of the covariance matrix by using Gerschgorin's theorem. Through these results and the properties of the CG method, we show that this method can find the MMSE-filter's output with far fewer iterations than the number of subcarriers. In addition, we propose a new preconditioning technique to speed up the convergence of the CG method at the expense of a small increase in complexity for each iteration; this technique is based on the fact that off-diagonal entries of the covariance matrix have smaller magnitude. To further reduce the

Manuscript received May 2, 2011; revised October 7, 2011 and February 22, 2012; accepted April 5, 2012. The associate editor coordinating the review of this paper and approving it for publication was G. Yue.

This work was supported in part by the National Research Foundation of Korea (NRF) grant funded by the Korea government (MEST) (No. 2010-0017909), and in part by the Seoul R&BD program (WR080951). The material in this paper was presented in part at IEEE ICC, June 2011.

K. Lee, S.-R. Lee, and I. Lee are with the School of Electrical Engineering, Korea University, Seoul, Korea (e-mail: {bachhi, sangrim78, inkyu}@korea.ac.kr).

S.-H. Moon is with the Electronics and Telecommunications Research Institute (ETRI), Daejeon, Korea (e-mail: sh.moon@etri.re.kr).

Digital Object Identifier 10.1109/TWC.2012.052512.110811

complexity, we introduce a way of implementing matrix-by-vector multiplications via fast Fourier transform (FFT) operations. As a result, CFO compensation can be obtained with significantly reduced computational complexity, while maintaining performance.

The paper is structured as follows: Section II introduces the signal model. In Section III, we apply the CG method for CFO compensation. Section IV presents several observations related to the convergence characteristics of the CG method. Section V discusses low-complexity implementations of the preconditioned CG method and compares the complexity with that of conventional schemes. In Section VI, simulation results are provided and Section VII concludes the paper.

Throughout this paper, normal letters represent scalar quantities, and boldface lower- and upper-case letters indicate vectors and matrices, respectively. We use $(\cdot)^T$, $(\cdot)^\dagger$, \otimes , $\langle \cdot \rangle_n$ and $\mathbb{E}[\cdot]$ to represent the transpose, complex conjugate transpose, Kronecker product, modulo n operation and expectation, respectively. In addition, $\|\cdot\|$ and $\det(\cdot)$ represent the 2-norm and the determinant, respectively. The subscripts $[\cdot]_k$ and $[\cdot]_{i,j}$ stand for the k -th element of a vector and the (i, j) -th entry of a matrix, respectively. \mathbf{I}_l denotes an identity matrix of size l . The minimum and maximum eigenvalues of \mathbf{A} are denoted as $\lambda_{\min}(\mathbf{A})$ and $\lambda_{\max}(\mathbf{A})$, respectively.

II. SIGNAL MODEL

In this paper, we consider uplink OFDMA systems with N subcarriers and K MUs. The CFO of the k -th MU is defined as ϵ_k which is normalized by the subcarrier spacing. In addition, the set \mathcal{C}_k represents the subcarrier indices of the k -th MU where $\mathcal{C}_k \cap \mathcal{C}_l = \emptyset$ for $k \neq l$. To simplify these presentation, we suppose that the cardinality of \mathcal{C}_k equals $P = \frac{N}{K}$. Let us define the channel impulse response vector \mathbf{h}_k as $\mathbf{h}_k = [h_{0,k} \ h_{1,k} \ \cdots \ h_{L-1,k}]^T$ where $h_{i,k}$ has an independent and identically distributed complex Gaussian distribution and L stands for the channel length. We denote $\mathbf{F} = [\mathbf{f}_0 \ \mathbf{f}_1 \ \cdots \ \mathbf{f}_{N-1}]$ as the $N \times N$ discrete Fourier transform (DFT) matrix with $\mathbf{f}_i = \frac{1}{\sqrt{N}} [1 \ e^{-j2\pi i} \ \cdots \ e^{-j2\pi i(N-1)}]^T$, and we define $\mathbf{F}_L = [\mathbf{f}_0 \ \mathbf{f}_1 \ \cdots \ \mathbf{f}_{L-1}]$. Then, the diagonal channel matrix \mathbf{H}_k is given as $\mathbf{H}_k = \sqrt{N} \text{diag}\{\mathbf{F}_L \mathbf{h}_k\} = \text{diag}\{H_{0,k}, H_{1,k}, \dots, H_{N-1,k}\}$ where $H_{i,k}$ is the channel gain of the i -th subcarrier for the k -th MU. Moreover, the transmitted signal of the k -th MU is obtained as $\mathbf{x}_k = [X_{0,k} \ X_{1,k} \ \cdots \ X_{N-1,k}]^T$ where $X_{m,k} = 0$ for $m \notin \mathcal{C}_k$ and $\mathbb{E}[|X_{m,k}|^2] = 1$ for $m \in \mathcal{C}_k$.

The received signal vector $\mathbf{r} = [r_0 \ r_1 \ \cdots \ r_{N-1}]^T$ after the cyclic prefix removal is computed as

$$\mathbf{r} = \sum_{k=1}^K \Gamma(\epsilon_k) \mathbf{F}^\dagger \mathbf{H}_k \mathbf{x}_k + \mathbf{w} \quad (1)$$

where $\Gamma(\epsilon_k) = \text{diag}\{1, e^{j\frac{2\pi\epsilon_k}{N}}, \dots, e^{j\frac{2\pi(N-1)\epsilon_k}{N}}\}$ represents a diagonal matrix whose diagonal entries stand for the phase shift of the corresponding received signal sample and $\mathbf{w} = [w_0 \ w_1 \ \cdots \ w_{N-1}]^T$ indicates the complex additive white Gaussian noise (AWGN) vector with zero mean and covariance matrix $\sigma_w^2 \mathbf{I}_N$.

Let us define a diagonal matrix Ψ_k as $[\Psi_k]_{i,i} = 1$ for $i \in \mathcal{C}_k$ and $[\Psi_k]_{i,i} = 0$ otherwise. For brevity, we denote the composite transmitted data for the MUs as $\mathbf{x} = \sum_{k=1}^K \Psi_k \mathbf{x}_k = [\bar{X}_0 \ \bar{X}_1 \ \cdots \ \bar{X}_{N-1}]$ where $\bar{X}_i = X_{i,k}$ for $i \in \mathcal{C}_k$. Similar to \mathbf{x} , the composite channel frequency-response is given as $\mathbf{H} = \sum_{k=1}^K \Psi_k \mathbf{H}_k = \text{diag}\{\bar{H}_0 \ \bar{H}_1 \ \cdots \ \bar{H}_{N-1}\}$ where $\bar{H}_i = H_{i,k}$ for $i \in \mathcal{C}_k$. Then, the DFT output of (1) is written as [13]

$$\begin{aligned} \bar{\mathbf{r}} &= \left(\sum_{k=1}^K \mathbf{C}(\epsilon_k) \Psi_k \right) \mathbf{H} \mathbf{x} + \bar{\mathbf{w}} \\ &= \mathbf{Q} \mathbf{u} + \bar{\mathbf{w}} \end{aligned} \quad (2)$$

where $\mathbf{C}(\epsilon_k) = \mathbf{F} \Gamma(\epsilon_k) \mathbf{F}^\dagger$ is a circulant matrix, $\mathbf{Q} = \sum_{k=1}^K \mathbf{C}(\epsilon_k) \Psi_k$ represents the *interference matrix*, and \mathbf{u} and $\bar{\mathbf{w}}$ denote $\mathbf{u} = \mathbf{H} \mathbf{x}$ and $\bar{\mathbf{w}} = \mathbf{F} \mathbf{w}$, respectively. The interference matrix \mathbf{Q} characterizes the normalized interference generated by multiple CFOs in the frequency domain, and the received signal vector $\bar{\mathbf{r}}$ is contaminated by the interference among subcarriers.

The least squares (LS) or MMSE criterion can be applied to suppress the interference among subcarriers on the basis of the estimated CFO of each MU at the uplink receiver [13]. As in [6]–[10], we assume that the CFOs¹ of all MUs are known at the base station. After the linear MMSE filter is applied, the CFO compensated signal is given by [6]

$$\hat{\mathbf{u}} = \left(\mathbf{Q}^\dagger \mathbf{Q} + \sigma_w^2 \mathbf{I}_N \right)^{-1} \mathbf{Q}^\dagger \bar{\mathbf{r}}. \quad (3)$$

Because the interference among subcarriers is minimized by the MMSE filter, we can detect \mathbf{x} from $\hat{\mathbf{u}}$ by using one-tap equalizer [16]. However, the computation of the MMSE filter requires an inverse operation of an $N \times N$ matrix as seen in (3). Thus, its required memory storage and computational complexity increase dramatically as N increases. To resolve the complexity and storage issues, we will employ the CG method as described in the following section.

III. IMPLEMENTATION OF THE CG METHOD

In this section, we adopt the CG method to obtain a solution $\hat{\mathbf{u}}$ for equation (3), which is rewritten as

$$\mathbf{M} \hat{\mathbf{u}} = \mathbf{b} \quad (4)$$

where we have $\mathbf{M} = \mathbf{Q}^\dagger \mathbf{Q} + \sigma_w^2 \mathbf{I}_N$ and $\mathbf{b} = \mathbf{Q}^\dagger \bar{\mathbf{r}}$. The procedure for solving (4) using the CG method is described in Algorithm 1. The superscript i denotes the iteration number, δ stands for the tolerance of the solution, and $\mathbf{g}^{(i)}$ and $\mathbf{d}^{(i)}$ are referred to as the residual vector and the search direction, respectively. Here, \mathbf{P} denotes the preconditioning matrix used to speed up the convergence of the CG method, which will be described in Section V. \mathbf{P} is assumed to be an identity matrix in Sections III and IV.

Note that this algorithm requires storage of only $\mathbf{g}^{(i)}$, $\mathbf{g}^{(i+1)}$ and $\mathbf{d}^{(i)}$. Thus, the total storage requirement is reduced. In contrast, the complexity reduction is not clear because \mathbf{M} is usually not a sparse matrix. In addition, the CG method may

¹In OFDMA systems, the CFOs can be estimated using the algorithms in [14] and [15].

Algorithm 1 CG algorithm

```

1:  $\mathbf{g}^{(0)} \leftarrow \mathbf{b} - \mathbf{M}\mathbf{u}^{(0)}$ 
2:  $\mathbf{d}^{(0)} \leftarrow \mathbf{P}^{-1}\mathbf{g}^{(0)}$ 
3: while  $\|\mathbf{g}^{(i)}\| > \delta\|\mathbf{g}^{(0)}\|$  do
4:    $\alpha^{(i)} \leftarrow \frac{\mathbf{g}^{(i)\dagger}\mathbf{P}^{-1}\mathbf{g}^{(i)}}{\mathbf{d}^{(i)\dagger}\mathbf{M}\mathbf{d}^{(i)}}$ 
5:    $\mathbf{u}^{(i+1)} \leftarrow \mathbf{u}^{(i)} + \alpha^{(i)}\mathbf{d}^{(i)}$ 
6:    $\mathbf{g}^{(i+1)} \leftarrow \mathbf{g}^{(i)} - \alpha^{(i)}\mathbf{M}\mathbf{d}^{(i)}$ 
7:    $\beta^{(i+1)} \leftarrow \frac{\mathbf{g}^{(i+1)\dagger}\mathbf{P}^{-1}\mathbf{g}^{(i+1)}}{\mathbf{g}^{(i)\dagger}\mathbf{P}^{-1}\mathbf{g}^{(i)}}$ 
8:    $\mathbf{d}^{(i+1)} \leftarrow \mathbf{P}^{-1}\mathbf{g}^{(i+1)} + \beta^{(i+1)}\mathbf{d}^{(i)}$ 
9: end while

```

require N iterations to obtain an exact solution². However, in the following section, we will show that the number of iterations needed to solve the CFO compensation problem in (4) is much less than the number of subcarriers.

IV. CONVERGENCE ANALYSIS

In this section, we analyze the convergence in two different CAS cases. First, for the ICAS, we present the maximum number of iterations required in the CG method to obtain an exact solution. Next, we derive an upper-bound of the eigenvalues of \mathbf{M} in the GCAS case to illustrate the convergence behavior of the CG method.

A. Description of \mathbf{Q} and \mathbf{M}

We first describe some preliminary mathematical results related to \mathbf{Q} and \mathbf{M} . Because $\mathbf{Q}^\dagger\mathbf{Q}$ is a positive-definite matrix, \mathbf{M} can be decomposed into

$$\mathbf{M} = \mathbf{Q}^\dagger\mathbf{Q} + \sigma_w^2\mathbf{I} = \mathbf{U}(\mathbf{\Lambda} + \sigma_w^2\mathbf{I})\mathbf{U}^\dagger \quad (5)$$

where \mathbf{U} is a unitary matrix and $\mathbf{\Lambda} = \text{diag}\{\lambda_1 \dots \lambda_N\}$ is a diagonal matrix whose diagonal entries denote the eigenvalues of $\mathbf{Q}^\dagger\mathbf{Q}$. Then, the n -th eigenvalue of \mathbf{M} is represented as $\lambda_n + \sigma_w^2$. To simplify the explanation, we neglect the noise for now and consider $\mathbf{M} = \mathbf{Q}^\dagger\mathbf{Q}$ below.

From (2), the entry $[\mathbf{Q}]_{a,b}$ is written as

$$\begin{aligned} [\mathbf{Q}]_{a,b} &= \frac{1}{N} \sum_{n=0}^{N-1} e^{j2\pi(\epsilon_g(b)+b)n/N} e^{-j2\pi an/N} \\ &= e^{j\pi(\epsilon_g(b)+b-a)(1-1/N)} \frac{\sin(\pi(\epsilon_g(b)+b-a))}{N\sin(\pi(\epsilon_g(b)+b-a)/N)} \end{aligned} \quad (6)$$

where $g(b)$ is equal to k for $b \in \mathcal{C}_k$. Note that each column of \mathbf{Q} is determined by the CFO of the corresponding user. Then, the (a,b) -th entry of \mathbf{M} is represented as

$$[\mathbf{M}]_{a,b} = \begin{cases} 1 & \text{for } b = a \\ 0 & \text{for } \epsilon_{g(a)} = \epsilon_{g(b)}, b \neq a \\ e^{j\theta_{a,b}} \frac{\sin \theta_{a,b}}{N \sin(\theta_{a,b}/N)} & \text{for } \epsilon_{g(a)} \neq \epsilon_{g(b)} \end{cases} \quad (7)$$

where $\theta_{a,b} = \pi(b-a + (\epsilon_{g(b)} - \epsilon_{g(a)}))$.

The second equation in (7) shows that the columns of \mathbf{Q} which belong to the same MU ($\epsilon_{g(a)} = \epsilon_{g(b)}$) are orthogonal

to each other. As a special case, if all the CFOs are the same, \mathbf{M} becomes an identity matrix. Moreover, the third equation in (7) shows that the magnitude of the off-diagonal entries is smaller than 1 and decreases as $\epsilon_{g(a)}$ approaches $\epsilon_{g(b)}$. For a general \mathbf{M} , the maximum eigenvalue is at least equal to or greater than 1 because $\sum_{n=1}^N \lambda_n = \sum_{n=1}^N [\mathbf{M}]_{n,n} = N$.

B. Convergence analysis for ICAS

In the ICAS, subcarriers allocated to each user are equally spaced in the entire frequency band [17]. By using this fact and equation (7), it is easy to show that \mathbf{M} is a Hermitian block-circulant matrix whose subblock size equals $K \times K$. An example of a Hermitian block-circulant matrix \mathbf{M} with $P = 4$ is represented as

$$\mathbf{M} = \begin{bmatrix} \mathbf{M}_1 & \mathbf{M}_2 & \mathbf{M}_3 & \mathbf{M}_2^\dagger \\ \mathbf{M}_2^\dagger & \mathbf{M}_1 & \mathbf{M}_2 & \mathbf{M}_3 \\ \mathbf{M}_3 & \mathbf{M}_2^\dagger & \mathbf{M}_1 & \mathbf{M}_2 \\ \mathbf{M}_2 & \mathbf{M}_3 & \mathbf{M}_2^\dagger & \mathbf{M}_1 \end{bmatrix}$$

where \mathbf{M}_i designates a subblock matrix of size $K \times K$. Here, \mathbf{M}_1 and \mathbf{M}_3 are Hermitian matrices.

It was shown in [18] that for a Hermitian block-circulant matrix, all distinct eigenvalues of \mathbf{M} are the same as those of $\mathbf{G}_1, \dots, \mathbf{G}_P \in \mathbb{C}^{K \times K}$, which is defined as

$$\mathbf{G}_t = \sum_{i=1}^P e^{-j2\pi(t-1)(i-1)/P} \mathbf{M}_i \quad \text{for } t = 1, 2, \dots, P. \quad (8)$$

As a result, we can find all eigenvalues of \mathbf{M} from \mathbf{G}_t , which is much smaller than \mathbf{M} when P is large. Using this observation, we now show the number of distinct eigenvalues of \mathbf{M} in the following lemma.

Lemma 1: For the ICAS, the number of distinct eigenvalues of \mathbf{M} is at most K .

Proof: By using the previously mentioned results and equations (7) and (8), \mathbf{G}_1 can be represented as

$$\mathbf{G}_1 = \mathbf{D}_2^\dagger \mathbf{G}_2 \mathbf{D}_2 = \mathbf{D}_3^\dagger \mathbf{G}_3 \mathbf{D}_3 = \dots = \mathbf{D}_P^\dagger \mathbf{G}_P \mathbf{D}_P$$

where $\mathbf{D}_t = \text{diag}\{\mathbf{d}_t\}$ with $[\mathbf{d}_t]_k = \exp\left(\frac{-j2\pi(t-1)(\epsilon_k - \epsilon_1 + k - 1)}{N}\right)$. Here, we easily confirm that \mathbf{D}_t is a unitary matrix with $\mathbf{D}_t^\dagger \mathbf{D}_t = \mathbf{D}_t \mathbf{D}_t^\dagger = \mathbf{I}_K$. Then, it is shown that \mathbf{G}_1 satisfies

$$\begin{aligned} \det(\mathbf{G}_1 - \lambda \mathbf{I}_K) &= \det(\mathbf{D}_t^\dagger \mathbf{G}_t \mathbf{D}_t - \lambda \mathbf{D}_t^\dagger \mathbf{D}_t) \\ &= \det(\mathbf{D}_t^\dagger) \det(\mathbf{G}_t - \lambda \mathbf{I}_K) \det(\mathbf{D}_t) \\ &= \det(\mathbf{G}_t - \lambda \mathbf{I}_K). \end{aligned}$$

Since the characteristic function of \mathbf{G}_1 is the same as that of \mathbf{G}_t for $t = 1, 2, \dots, P$, the number of distinct eigenvalues of \mathbf{M} is at most K not N . ■

Since the number of iterations required for the CG method to obtain an exact solution is at most the number of distinct eigenvalues [11] [12], we see from Lemma 1 that for the ICAS with K MUs, an exact solution can be found within K iterations. Meanwhile, the paper in [19] showed that if a matrix is block-circulant, the inverse matrix is also block-circulant and can be computed in a closed-form with $O(NK^3)$. Nevertheless, its complexity is higher than that of

²For a positive definite matrix with size N , the CG method is in principle guaranteed to converge and can find an exact solution within N iterations [11].

the CG method. However, this method may be useful when an explicit expression of \mathbf{M}^{-1} is required. Note that the CG method provides only a solution of the inverse problem.

C. Convergence analysis for GCAS

In contrast to the ICAS, the GCAS allows each MU to select subcarriers according to its quality of service (QoS) and channel conditions [20]. Thus, it is impossible to characterize the structure of \mathbf{M} , and the characteristic function for \mathbf{M} cannot be expressed in a closed-form, unlike that in the ICAS. Meanwhile, the authors in [21] showed that the clustering of eigenvalues affects the convergence rate of the CG method. Therefore, in what follows, we derive an upper-bound of the maximum eigenvalue of \mathbf{M} to show the convergence behavior of the CG method in the GCAS.

Lemma 2: The maximum eigenvalue of \mathbf{M} is upper bounded as

$$\lambda_{\max}(\mathbf{M}) \leq \max_r \left\{ \frac{1}{N} \sum_{c=1}^N \left| \frac{\sin \theta_{r,c}}{\sin \frac{\theta_{r,c}}{N}} \right| \right\} \triangleq \lambda_{\text{up}}(\mathbf{M}) \quad (9)$$

where the equality holds only when all the CFOs are the same.

Proof: By using Gerschgorin's theorem in [22], the maximum eigenvalue of \mathbf{M} satisfies the following inequality

$$|\lambda_{\max}(\mathbf{M}) - 1| \leq \max_r \sum_{c \neq r} |[\mathbf{M}]_{r,c}|. \quad (10)$$

Since the maximum eigenvalue is equal to or greater than 1, we can simplify equation (10) as

$$\lambda_{\max}(\mathbf{M}) \leq 1 + \max_r \sum_{c \neq r} |[\mathbf{M}]_{r,c}| = \max_r \sum_{c=1}^N |[\mathbf{M}]_{r,c}|.$$

From (7), we complete the proof. ■

It can be seen from (9) that $\lambda_{\text{up}}(\mathbf{M})$ is a function of the CFOs and the subcarrier indices of all MUs. To obtain an upper-bound that is independent of the CFOs and the subcarrier indices, we compute the maximum among the upper-bounds as follows.

Corollary 1: The maximum of $\lambda_{\text{up}}(\mathbf{M})$ in (9) can be approximated by

$$\max_{\substack{\{\epsilon_1, \dots, \epsilon_K\} \\ \{c_1, \dots, c_K\}}} \lambda_{\text{up}}(\mathbf{M}) \lesssim 2 + \sum_{t=2}^{N-1} \frac{1}{\pi(t-1/2)}. \quad (11)$$

Proof: See Appendix A. ■

Fig. 1 presents the maximum of $\lambda_{\text{up}}(\mathbf{M})$ in (11) and the largest eigenvalues of \mathbf{M} ($\sigma_w^2 = 0$), which are obtained from simulation with different numbers of subcarriers. We can see that both $\lambda_{\max}(\mathbf{M})$ and $\max\{\lambda_{\text{up}}(\mathbf{M})\}$ are much smaller than N and increase slowly with N , which indicates that all the eigenvalues are distributed in a very narrow range $[0, \max\{\lambda_{\text{up}}(\mathbf{M})\}]$. In particular, it can be seen from Gerschgorin's theorem that most of the eigenvalues are clustered near the center of 1, because all the diagonal entries of \mathbf{M} are equal to 1. Note that the CG method finds a solution more quickly when eigenvalues are clustered [11] [21]. As a result, for the GCAS, the CG method can compute the MMSE solution in (3) with a few iterations even for large N , which will be shown in Section VI.

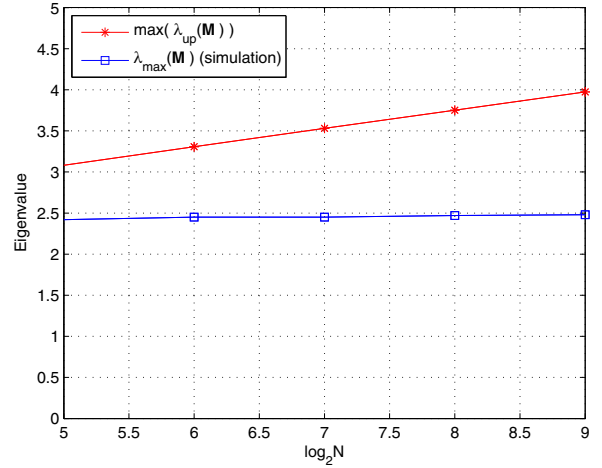


Fig. 1. Upper bound of maximum eigenvalues.

V. IMPLEMENTATION OF PRECONDITIONED CG METHOD

Preconditioning is a technique for accelerating the convergence of the CG method by clustering the eigenvalues of a matrix [11]. For symmetric positive definite matrices, incomplete Cholesky factorization (ICF) has been a general method of obtaining a preconditioner, and several ICF algorithms have been reported in [23]–[26]. For our case, let us define $\hat{\mathbf{L}}$ as the incomplete Cholesky factor of \mathbf{M} . Then, the preconditioned matrix $\hat{\mathbf{L}}^{-1}\mathbf{M}(\hat{\mathbf{L}}^{-1})^\dagger$ is expected to have more clustered eigenvalues with the improved conditional number³, which speeds up the convergence of the CG method [11]. If $\mathbf{P} = \hat{\mathbf{L}}\hat{\mathbf{L}}^\dagger$ is used as a preconditioner in Algorithm 1, we call this CG method as the preconditioned CG (PCG) method.

A. Low-complexity implementation of the preconditioning

Although preconditioning via the incomplete Cholesky factor is a well known technique, there are two issues to consider for our problem. First, for the ICF algorithm, an explicit expression of \mathbf{M} is necessary, but it requires a matrix-by-matrix multiplication as $\mathbf{Q}^\dagger\mathbf{Q}$. Moreover, a sparse matrix is preferable when the ICF algorithm computes $\hat{\mathbf{L}}$ from \mathbf{M} . However, \mathbf{M} is fully dense in most cases. In this case, the conventional ICF algorithm requires a computational complexity of at most $O(N^3)$. To overcome these problems, in this subsection, we describe a low-complexity implementation of the preconditioning.

Since $\hat{\mathbf{L}}$ is already incomplete, an exact computation of \mathbf{M} is not required. For this reason, we first define $\hat{\mathbf{Q}}$ as a sparse \mathbf{Q} having a few non-zero elements. Based on the fact that the interference power caused by one subcarrier to another subcarrier decreases as the distance between the two subcarriers increases, we can approximate \mathbf{Q} as a banded matrix [6]

$$[\hat{\mathbf{Q}}]_{a,b} = 0, \quad \text{for } \langle a-b \rangle_N > B \quad \text{and} \quad \langle b-a \rangle_N > B \quad (12)$$

³The conditional number of a matrix \mathbf{A} is defined as $\lambda_{\max}(\mathbf{A})/\lambda_{\min}(\mathbf{A})$. For the CG method, the smaller the conditional number is, the more rapidly it converges.

where B denotes the band-width of $\hat{\mathbf{Q}}$. Thus, the number of non-zero elements in $\hat{\mathbf{Q}}$ is at most $(2B + 1)N$. For example, a banded matrix with $N = 5$ and $B = 1$ is given as

$$\hat{\mathbf{Q}} = \begin{bmatrix} \times & \times & 0 & 0 & \times \\ \times & \times & \times & 0 & 0 \\ 0 & \times & \times & \times & 0 \\ 0 & 0 & \times & \times & \times \\ \times & 0 & 0 & \times & \times \end{bmatrix}.$$

Note that B can be set to a value much smaller than N when N is large. Then, an incomplete matrix of \mathbf{M} , denoted by $\bar{\mathbf{M}}$, can be made from $\hat{\mathbf{Q}}$; in this case, the complexity is reduced from $O(N^3)$ to $O(N(2B+1)^2)$. Further, considering that each off-diagonal entry of \mathbf{M} in (7) has an expression similar to that in (6), $\bar{\mathbf{M}}$ can also be approximated by a banded matrix, denoted by $\hat{\mathbf{M}}$, where zero entries are determined by the same condition as in (12), and the band-width is denoted by S .

Algorithm 2 Modified ICF algorithm

```

1: for  $j = 1 : N$ 
2:    $[\hat{\mathbf{M}}]_{j,j} \leftarrow \sqrt{[\hat{\mathbf{M}}]_{j,j}}$ 
3:   for  $i = \min(j + 1, N) : N$ 
4:      $b \leftarrow [\hat{\mathbf{M}}]_{i,i} - |[\hat{\mathbf{M}}]_{i,j}|^2$ 
5:     if  $b > 0$ 
6:        $[\hat{\mathbf{M}}]_{i,i} \leftarrow b$ 
7:   end
8: end
9:  $\hat{\mathbf{L}} \leftarrow$  lower triangular part of  $\hat{\mathbf{M}}$ 

```

To obtain $\hat{\mathbf{L}}$ from the banded matrix $\hat{\mathbf{M}}$, we suggest the modified ICF algorithm described in Algorithm 2; this algorithm is developed on the basis of $\hat{\mathbf{M}}$ being a banded matrix. It can be seen that Algorithm 2 contains only *two loops*⁴, and only diagonal elements of $\hat{\mathbf{M}}$ are updated, unlike the case in conventional ICF algorithms, which considerably decreases the complexity. In addition, the second loop in Algorithm 2 can be quickly terminated or omitted, because $\hat{\mathbf{M}}$ is a sparse banded matrix. Note that for a dense matrix, conventional ICF algorithms should compute all the entries of the matrix and determine whether the computed entries are discarded or updated, which makes the operation highly complex.

Now we consider the complexity when the operation $\mathbf{P}^{-1}\mathbf{g}^{(i)}$ is performed in Algorithm 1. Note that $\mathbf{P}^{-1}\mathbf{g}^{(i)}$ can be computed by two back substitutions, because $\mathbf{P}^{-1} = (\hat{\mathbf{L}}^{-1})^\dagger \hat{\mathbf{L}}^{-1}$ with a lower triangular matrix $\hat{\mathbf{L}}$. In this case, if $\hat{\mathbf{L}}$ has only a few non-zero elements, the complexity of the back substitution is reduced. Hence, we allow no fill-in⁵ in order to obtain a sparse $\hat{\mathbf{L}}$. Namely, after calculating $\hat{\mathbf{L}}$ in Algorithm 2, the entries of $\hat{\mathbf{L}}$ that correspond to the position of zeros in the original matrix $\hat{\mathbf{M}}$ are discarded [24]–[26]. Then, $\hat{\mathbf{L}}$ also becomes a banded matrix with the same band-width S as $\hat{\mathbf{M}}$. As a result, the number of complex multiplications required to calculate $\hat{\mathbf{L}}$ and perform two back substitutions is $\frac{N}{2}(K \log_2 N + (2B + 1)^2 + (B + 1))$ and $2(S + 1)N$, respectively.

⁴The conventional ICF algorithms in [24]–[26] contain *three loops*.

⁵With no fill-in, the sparsity pattern of $\hat{\mathbf{L}}$ is set to that of the original matrix $\hat{\mathbf{M}}$ [24]–[26].

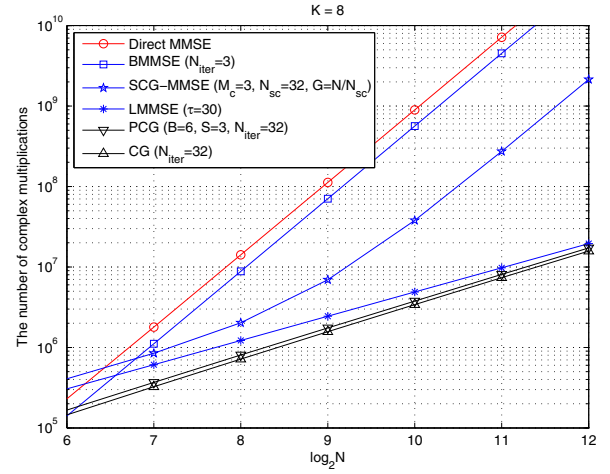


Fig. 2. Computational loads of CFO compensation algorithms.

TABLE I
COMPLEX MULTIPLICATIONS OF CFO COMPENSATION ALGORITHMS

Direct MMSE	$O(N^3)$	BMMSE	$O(N_{\text{iter}}N^3/K)$
SCG-MMSE	$O(M_cGN^2)$	CG	$O(N_{\text{iter}}(KN \log_2 N))$
LMMSE	$O(5N\tau^2)$	PCG	$O(N_{\text{iter}}(KN \log_2 N))$

B. Low complexity implementation via FFT operations

For a low-complexity implementation, we rewrite $\mathbf{M}\mathbf{d}^{(i)}$ in Algorithm 1 as

$$\begin{aligned} \mathbf{M}\mathbf{d} &= (\mathbf{Q}^\dagger \mathbf{Q} + \sigma_w \mathbf{I}_N) \mathbf{d} \\ &= \sum_{k=1}^K \Psi_k \mathbf{F} \Gamma^\dagger(\epsilon_k) \sum_{l=1}^K \Gamma(\epsilon_l) \mathbf{F}^\dagger \Psi_l \mathbf{d} + \sigma_w \mathbf{d} \quad (13) \end{aligned}$$

where the superscript i is omitted from $\mathbf{d}^{(i)}$ for brevity. From (13), we see that multiplications between $\mathbf{Q}^\dagger \mathbf{Q}$ and \mathbf{d} can be implemented with $2K$ FFT operations and $2K$ vector-by-vector multiplications. Hence, the computational complexity $O(N^2)$ can be reduced to $O(KN \log_2 N)$.

For the ICAS, in particular, the complexity can be further reduced by using the method in [17]. Defining the vector whose elements correspond to nonzero elements of $\Psi_l \mathbf{d}$ as $\tilde{\mathbf{d}}$, we have

$$\mathbf{F}^\dagger \Psi_l \mathbf{d} = \Gamma(l-1) (\mathbf{I}_K \otimes (\tilde{\mathbf{F}}^\dagger \tilde{\mathbf{d}}))$$

where $\tilde{\mathbf{F}}^\dagger$ is the inverse DFT matrix of size P and $\Gamma(l-1) = \text{diag}\{1, e^{j2\pi(l-1)/N}, \dots, e^{j2\pi(l-1)(N-1)/N}\}$. As a result, we can employ the inverse FFT operation of size P instead of N . However, $\Psi_k \mathbf{F} \Gamma^\dagger(\epsilon_k)$ still requires the $N \times N$ FFT operations.

Fig. 2 illustrates the computational complexity of the CG and PCG methods and other schemes according to the number of subcarriers. For a fair comparison, we consider the computational complexity required for the GCAS. Here, we assume $K = 8$ and $P = N/K$ where N_{iter} denotes the number of iterations. For the SCG-MMSE, M_c , G and N_{sc} represent the number of IC units, groups and subcarriers per group, respectively. Further, for the LMMSE, τ indicates the band-width of a matrix. In addition, we refer to the subblock-based MMSE scheme in [9] as BMMSE. The Direct MMSE

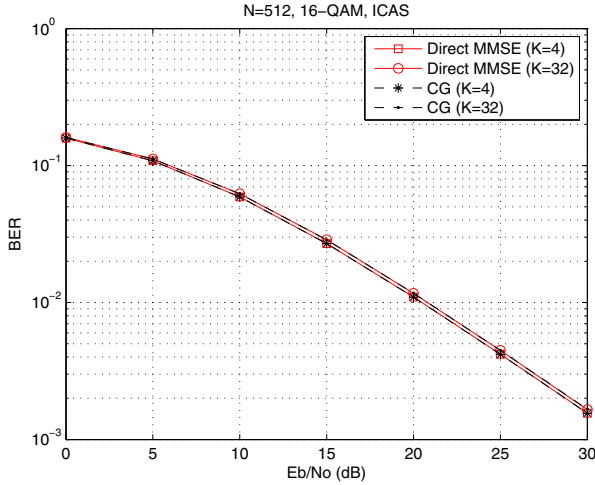


Fig. 3. BER of Direct MMSE and CG for ICAS.

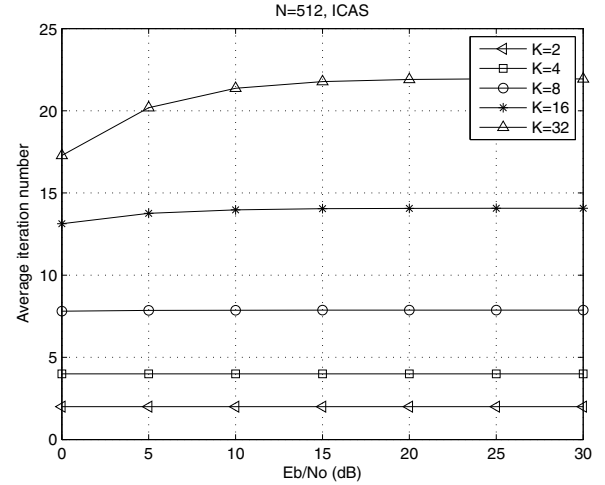


Fig. 4. Average iteration number of CG for ICAS.

includes an inverse operation for direct computation of the corresponding filter. Fig. 2 shows that the CG and PCG methods exhibit the lowest complexity, whereas the Direct MMSE, BMMSE and SCG-MMSE methods have steep slopes with respect to N . This can also be verified from Table I where the former have a complexity of $O(N_{\text{iter}}KN \log N)$, whereas the complexity of the latter increases to $O(N^3)$. Note that the actual size of N in practical OFDMA systems such as WiMAX and 3GPP LTE ranges from 128 to 2048. The LMMSE has slightly higher computational complexity than the CG method, but simulation results show that it yields saturated BER performance in regions of moderate and high signal-to-noise ratio (SNR). As a result, the CFO compensation in (3) can be implemented with substantially reduced computational complexity by using the CG and PCG methods.

VI. SIMULATION RESULTS

In this section, we present the BER performance and iteration number of the CG and PCG methods and compare them with those of conventional schemes in OFDMA uplink systems with $N = 512$ subcarriers. We assume a 5-tap Rayleigh fading exponentially decaying channel with 16-QAM and 3,000 simulation runs. $\{\epsilon_1, \dots, \epsilon_K\}$ are chosen independently from a uniform distribution within the range $[-0.5, 0.5]$ which guarantees that \mathbf{Q} is a full rank matrix [6]. For the GCAS, P subcarriers are randomly assigned to each user. Unless stated otherwise, the tolerance δ and N_{iter} of the CG and the PCG methods are set to 10^{-4} and 32, respectively. Note that the values of δ and N_{iter} are determined such that the PCG method achieves the performance of the Direct MMSE at $E_b/N_o = 30$ dB. In addition, an all-zero vector is used as the initial estimate $\mathbf{u}^{(0)}$.

Fig. 3 compares the BER performance of the CG method with that of the Direct MMSE for the ICAS. To verify Lemma 1, N_{iter} is set to K . We see that the BER performance of the CG method is identical to that of the Direct MMSE. Consequently, for the ICAS, N_{iter} can be set to K without any performance loss. In this case, the computational complexity

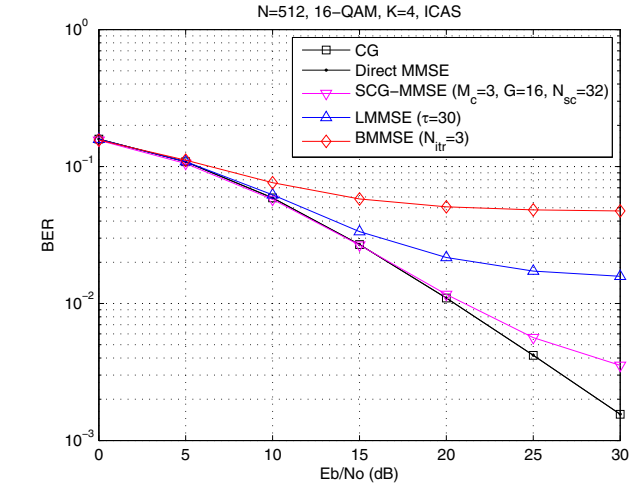


Fig. 5. BER of CG and conventional schemes for ICAS.

of the CG method is given by $O(K^2N \log N)$, whereas that of the Direct MMSE⁶ is $O(N(N+K^3))$. Therefore, the required complexity of the former is much lower than that of the latter.

Fig. 4 presents the average iteration number of the CG method for the ICAS. We see that the average iteration number for $K = 32$ is much smaller than 32, which indicates that a solution that satisfies $\delta \leq 10^{-4}$ is found within 32 iterations. Hence, the average computational complexity of the CG is much less than that presented in Fig. 2 which accounts for the worst complexity. Moreover, it can be seen that the average iteration number decreases at low SNR. This is because at low SNR, the noise variance σ_w^2 in (5) prevents the conditional number from being very large even if $\lambda_{\min}(\mathbf{Q}^\dagger \mathbf{Q})$ is very small⁷.

Fig. 5 compares the BER of the CG method and the conventional schemes for the ICAS with $K = 4$. The conventional schemes yield degraded performance in the high SNR region

⁶The complexities for obtaining \mathbf{M}^{-1} and $\hat{\mathbf{u}} = \mathbf{M}^{-1}\mathbf{b}$ are $O(NK^3)$ and N^2 , respectively.

⁷From (5), the conditional number of \mathbf{M} is defined as $\frac{\lambda_{\max}(\mathbf{Q}^\dagger \mathbf{Q}) + \sigma_w^2}{\lambda_{\min}(\mathbf{Q}^\dagger \mathbf{Q}) + \sigma_w^2}$.

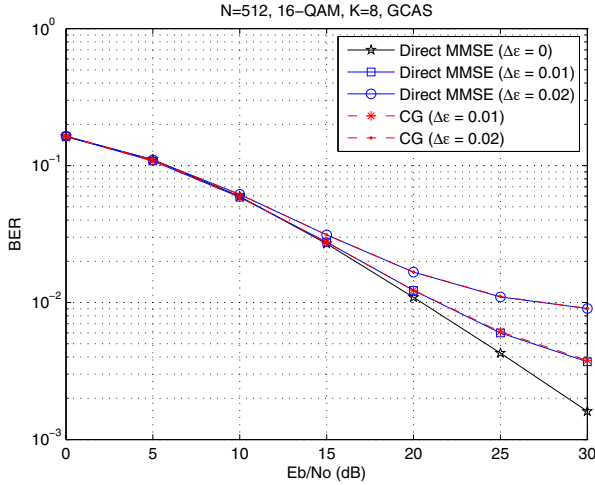


Fig. 6. BER of CG and Direct MMSE for GCAS in the presence of the CFO estimation error.

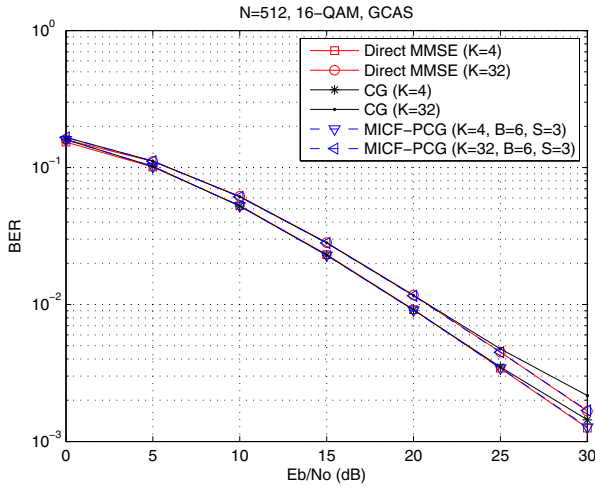


Fig. 7. BER comparison of different schemes for GCAS.

unlike the CG method. This can be explained by the fact that the conventional schemes were developed on the basis of the approximated signal model in order to reduce the complexity.

Fig. 6 shows the BER performance of the CG and the Direct MMSE in the presence of the CFO estimation error denoted by $\Delta\epsilon$. Thus, the interference matrix \mathbf{Q} in (3) and $\mathbf{M}\mathbf{d}^{(i)}$ in (13) are generated using CFOs of $\epsilon_k + \Delta\epsilon$. As in Fig. 3, the CG method has almost the same performance as the Direct MMSE in all SNR regions regardless of $\Delta\epsilon$. This is due to the fact that a solution of the CG method becomes essentially identical to that of the Direct MMSE after N iterations.

Next, we compare the BER and average iteration number of the PCG with those of the CG in the GCAS to demonstrate the improved convergence obtained by using our proposed preconditioner. Fig. 7 illustrates the BER performance of the CG and the PCG methods for the GCAS. Here, the tolerance changes depending on the SNR as $\delta = \frac{\sigma_w^2}{10}$. In addition, σ_w^2 is set to 10^{-3} when $\sigma_w^2 < 10^{-3}$. To show the efficacy of the modified ICF with the banded matrices $\hat{\mathbf{M}}$ and $\hat{\mathbf{L}}$, we compare it with the conventional ICF described in [24]. For

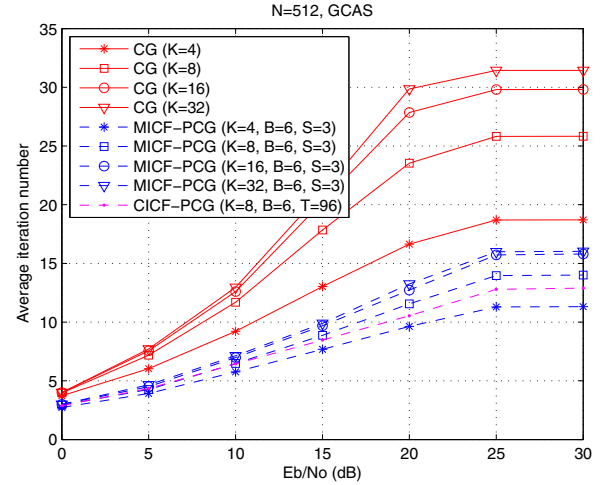


Fig. 8. Average iteration number of CG and PCG for GCAS.

simplicity, we refer to the PCG methods aided by the modified ICF and conventional ICF as MICF-PCG and CICF-PCG, respectively. Moreover, for the CICF, $\hat{\mathbf{L}}$ is obtained from $\hat{\mathbf{M}}$ not $\hat{\mathbf{M}}$. The CG method exhibits almost the same performance as the Direct MMSE in the low and moderate SNR regions with iterations much smaller than 512. However, for a large K , the CG method exhibits a slight BER performance loss at high SNR because of the limitation on N_{iter} . In contrast, the MICF-PCG yields almost the same performance as the Direct MMSE for the entire SNR range.

Fig. 8 shows the average iteration number of the CG and PCG methods for different numbers of MUs. The design parameter⁸ T in Fig. 8 indicates the maximum number of allowable non-zero elements in each column of $\hat{\mathbf{L}}$ [24]. For the CG method, the average iteration number increases as K grows. In contrast, in MICF-PCG, the average iteration number does not grow much with K , while the performance is maintained. In particular, for $K = 32$, its average iteration number is similar to that for $K = 16$. This indicates that we do not need to set a large N_{iter} to prevent a performance loss at high SNR even with a large number of MUs. For $K = 8$, the MICF-PCG has a slightly higher average iteration number than the CICF-PCG with $T = 96$, although the computational complexity of the CICF is much higher than that of the MICF. Therefore, we can confirm that our proposed preconditioner approximates \mathbf{M} well enough to improve convergence with a small increase in complexity.

On the other hand, the average iteration number is reduced as the SNR decreases, while the performance of the Direct MMSE is achieved. This can be explained by the fact that the residual error⁹ of the CG is masked by the noise in low and moderate SNR regions. Thus, we can further reduce the iteration numbers by adaptively adjusting the tolerance level. Note that the computational complexity of the CG presented in Fig. 2 is computed for $N_{\text{iter}} = 32$. In conclusion, the

⁸Note that the iteration number of the CG method decreases as T becomes large, but the increased complexity required to compute $\hat{\mathbf{L}}$ and perform the back substitution increases.

⁹The residual error vector is defined as $\mathbf{r} - \mathbf{M}\mathbf{u}^{(i)}$, and it becomes a zero vector after N iterations.

CG method, in conjunction with the proposed preconditioner and an adaptive tolerance, can produce almost the same BER performance as the Direct MMSE with a significantly reduced computational complexity even for large K .

VII. CONCLUSION

In this paper, we proposed a solution based on the CG method that minimizes the computational complexity required to compensate the CFO. To assess the efficacy of the CG method for addressing this problem, we analyzed the interference matrix and presented several observations that provide insights on the convergence rate of the CG method. Our analysis and simulation results show that the CG method converges to a solution with far fewer iterations than the number of subcarriers and can be implemented by FFT operations. Further, the CG method aided by the proposed preconditioner finds a solution with far fewer iterations than the number of subcarriers even for large N and K , although the complexity for each iteration increases slightly. As a result, CFO compensation can be achieved with a significantly reduced computational complexity.

APPENDIX

A. Proof of Corollary 1

To obtain an upper-bound independent of the CFOs and the subcarrier indices, we compute the maximum of the upper-bounds as

$$\begin{aligned} \max_{\substack{\{\epsilon_1, \dots, \epsilon_K\} \\ \{c_1, \dots, c_K\}}} \lambda_{\text{up}}(\mathbf{M}) &= \max_{\substack{\{\epsilon_1, \dots, \epsilon_K\} \\ \{c_1, \dots, c_K\}}} \max_r \frac{1}{N} \sum_{c=1}^N \left| \frac{\sin \theta_{r,c}}{\sin \frac{\theta_{r,c}}{N}} \right| \\ &\leq \max_{\{\epsilon_1, \dots, \epsilon_N\}} \max_r \frac{1}{N} \sum_{c=1}^N \left| \frac{\sin \pi(c-r+(\epsilon_c-\epsilon_r))}{\sin \frac{\pi(c-r+(\epsilon_c-\epsilon_r))}{N}} \right| \end{aligned} \quad (14)$$

where (14) comes from $\max_{\substack{\{\epsilon_1, \dots, \epsilon_K\} \\ \{c_1, \dots, c_K\}}} \lambda_{\text{up}}(\mathbf{M}) \leq \max_{\substack{\{\epsilon_1, \dots, \epsilon_N\} \\ \{c_1, \dots, c_N\}}} \lambda_{\text{up}}(\mathbf{M})$ and $r \in \{1, 2, \dots, N\}$. For $K = N$, we have $\mathcal{C}_c = \{c\}$ and $\epsilon_{g(c)} = \epsilon_c$. Without loss of generality, r is set to 1. Then, we define $\Phi(\nu_t)$ as

$$\Phi(\nu_t) = \frac{1}{N} \left| \frac{\sin \pi(t + \nu_t)}{\sin \frac{\pi(t + \nu_t)}{N}} \right|$$

where $t = c - 1$ and $\nu_t = \epsilon_{t+1} - \epsilon_1$. Note that ν_t is distributed within the range $[-1, 1)$.

Therefore, (14) can be evaluated as

$$\begin{aligned} \max_{\substack{\{\epsilon_1, \dots, \epsilon_K\} \\ \{c_1, \dots, c_K\}}} \lambda_{\text{up}}(\mathbf{M}) &\leq |\Phi(\nu_0)| + \max_{\nu_1} |\Phi(\nu_1)| \\ &\quad + \max_{\{\nu_2, \dots, \nu_{N-1}\}} \sum_{t=2}^{N-1} |\Phi(\nu_t)| \\ &= 2 + \max_{\{\nu_2, \dots, \nu_{N-1}\}} \sum_{t=2}^{N-1} |\Phi(\nu_t)| \end{aligned} \quad (15)$$

$$\approx 2 + \max_{\{\nu_2, \dots, \nu_{N-1}\}} \sum_{t=2}^{N-1} \left| \frac{\sin \pi(t + \nu_t)}{\pi(t + \nu_t)} \right| \quad (16)$$

where (15) results from the fact that $\max_{\nu_1} \{|\Phi(\nu_1)|\} = 1$ when $\nu_1 = -1$ ($t = 1$), and $|\Phi(\nu_0)| = 1$. Also, we approximate $\Phi(\nu_t) = \frac{\sin \pi(t + \nu_t)}{N \sin \frac{\pi(t + \nu_t)}{N}}$ in (16) as $\tilde{\Phi}(\nu_t) = \frac{\sin \pi(t + \nu_t)}{\pi(t + \nu_t)}$.

Here, $|\tilde{\Phi}(\nu_t)|$ has the largest magnitude when ν_t satisfies $\frac{1}{\pi} \tan(\pi \nu_t) - \nu_t = t$ for $\nu_t \in [-1, 1)$, but its closed-form solution is not available. However, the solution ν_t converges asymptotically to $-\frac{1}{2}$ as t increases, since $\nu_t = \frac{1}{\pi} \arctan(\pi t)$ for $t \rightarrow \infty$. In addition, the maximum of $|\tilde{\Phi}(\nu_t)|$ has a similar magnitude¹⁰ of $|\tilde{\Phi}(\nu_t = -\frac{1}{2})|$ even for small t . As a result, equation (16) can be simply upper bounded as

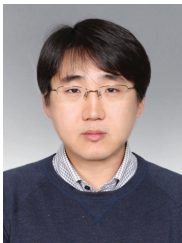
$$\max_{\substack{\{\epsilon_1, \dots, \epsilon_K\} \\ \{c_1, \dots, c_K\}}} \lambda_{\text{up}}(\mathbf{M}) \lesssim 2 + \sum_{t=2}^{N-1} \frac{1}{\pi(t-1/2)}.$$

REFERENCES

- [1] "IEEE standard for local and metropolitan area networks, part 16: air interface for fixed and mobile broadband wireless access systems amendment 2: physical and medium access control layers for combined fixed and mobile operation in licensed bands," IEEE Std. 802.16e, Feb. 2006.
- [2] K. Etemad, "Overview of mobile WiMAX technology and evolution," *IEEE Commun. Mag.*, vol. 46, pp. 31–40, Oct. 2008.
- [3] C. Y. Wong, R. S. Cheng, K. B. Letaief, and R. D. Murch, "Multicarrier OFDM with adaptive subcarrier, bit, and power allocation," *IEEE J. Sel. Areas Commun.*, vol. 17, pp. 479–483, Oct. 1999.
- [4] J. Lee, H.-L. Lou, and D. Toumpakaris, "Effect of carrier frequency offset on OFDM systems for multipath fading channels," in *Proc. 2004 IEEE GLOBECOM*, vol. 6, pp. 3721–3725.
- [5] T. Pollet, M. V. Bladel, and M. Moeneclaey, "BER sensitivity of OFDM systems to carrier frequency offset and Wiener phase noise," *IEEE Trans. Commun.*, vol. 43, pp. 191–193, Feb./Mar./Apr. 1995.
- [6] Z. Cao, U. Tureli, and Y.-D. Yao, "Low-complexity orthogonal spectral signal construction for generalized OFDMA uplink with frequency synchronization errors," *IEEE Trans. Veh. Technol.*, vol. 56, pp. 1143–1154, May 2007.
- [7] D. Huang and K. B. Letaief, "An interference-cancellation scheme for carrier frequency offsets correction in OFDMA systems," *IEEE Trans. Commun.*, vol. 53, pp. 1155–1165, July 2005.
- [8] T. Yucek and H. Arslan, "Carrier frequency offset compensation with successive cancellation in uplink OFDMA systems," *IEEE Trans. Wireless Commun.*, vol. 6, pp. 3546–3551, Oct. 2007.
- [9] G. Chen, Y. Zhu, and K. B. Letaief, "Combined MMSE-FDE and interference cancellation for uplink SC-FDMA with carrier frequency offsets," in *Proc. 2010 IEEE ICC*, pp. 1–5.
- [10] R. Fa and L. Zhang, "A generalized subcarrier-grouped MMSE based multi-stage interference cancellation scheme for OFDMA uplink systems with CFOs," in *Proc. 2010 IEEE ISWCS*, pp. 912–916.
- [11] J. R. Shewchuk, *An Introduction to the Conjugate-Gradient Method Without the Agonizing Pain*. Carnegie Mellon University, School of Computer Science, 1994.
- [12] O. Axelsson, "Iteration number for the conjugate gradient method," *Mathematics and Computers in Simulation*, vol. 61, pp. 421–435, Jan. 2003.
- [13] Z. Cao, U. Tureli, Y.-D. Yao, and P. Honan, "Frequency synchronization for generalized OFDMA uplink," in *Proc. 2004 IEEE GLOBECOM*, vol. 2, pp. 1071–1075.
- [14] Y. Na and H. Minn, "Line search based iterative joint estimation of channels and frequency offsets for uplink OFDMA systems," *IEEE Trans. Wireless Commun.*, vol. 6, pp. 4374–4382, Dec. 2007.
- [15] K. Lee, S.-H. Moon, and I. Lee, "Low-complexity leakage-based carrier frequency offset estimation techniques for OFDMA uplink systems," in *Proc. 2010 IEEE GLOBECOM*, pp. 1–5.
- [16] H. Sari, G. Karam, and I. Jeanclaude, "Transmission techniques for digital terrestrial TV broadcasting," *IEEE Commun. Mag.*, pp. 100–109, Feb. 1995.
- [17] Z. Cao, U. Tureli, and Y.-D. Yao, "Deterministic multiuser CFO estimation for interleaved OFDMA uplink," *IEEE Trans. Commun.*, vol. 52, pp. 1585–1594, Sep. 2004.
- [18] G. J. Tee, "Eigenvectors of block circulant and alternating circulant matrices," *New Zealand J. Mathematics*, vol. 36, pp. 195–211, 2007.
- [19] T. D. Mazancourt and D. Gerlic, "The inverse of a block-circulant matrix," *IEEE Trans. Antennas Propag.*, vol. 31, pp. 808–810, Sep. 1983.

¹⁰For $t = 2$, the maximum of $|\tilde{\Phi}(\nu_2)|$ and $|\tilde{\Phi}(\nu_2 = -\frac{1}{2})|$ are equal to 0.217 and 0.212, respectively.

- [20] Z. Wang, Y. Xin, and G. Mathew, "Iterative carrier-frequency offset estimation for generalized OFDMA uplink transmission," *IEEE Trans. Wireless Commun.*, vol. 8, pp. 1373–1383, Mar. 2009.
- [21] V. Iu, L. Lamas, Y. Li, and K. M. Mok, *Computational Methods in Engineering and Science*. Aa Balkema, 2004.
- [22] R. A. Horn and C. R. Johnson., *Matrix Analysis*. Cambridge University Press, 1990.
- [23] M. T. Jones and P. E. Plassmann, "An improved incomplete Cholesky factorization," *ACM Trans. Mathematical Software*, vol. 21, Mar. 1995.
- [24] C.-J. Lin and J. J. More, "Incomplete Cholesky factorizations with limited memory," *Society for Industrial and Applied Mathematics*, vol. 21, pp. 24–45, 1999.
- [25] T. Huang, Y. Zhang, and L. Li, "Modified incomplete Cholesky factorization for solving electromagnetic scattering problems," *Progress in Electromagnetics Research*, vol. 13, pp. 41–58, 2009.
- [26] Y. Saad, *Iterative Methods for Sparse Linear Systems*. Society for Industrial and Applied Mathematics, 2000.



Kilbom Lee (S'10) received the B.S. and M.S. degrees in electrical engineering from Korea University, Seoul, Korea in 2006 and 2009, respectively. He is currently working toward the Ph.D. degree at Korea University, Seoul, Korea. During the spring in 2010, he visited University of Southern California, Los Angeles, CA, to conduct collaborative research under the Brain Korea 21 (BK21) Program. His research interests are in wireless communication theory with synchronization algorithms for multiple-access communication systems and signal processing techniques for MIMO wireless cellular networks.



Sang-Rim Lee (S'05) received the B.S. and M.S. degrees in electrical engineering from Korea University, Seoul, Korea, in 2005 and 2007. From 2007 to 2010, he was a research engineer in the Samsung Electronics, where he conducted research on WiMAX system. Currently, he is working toward the Ph.D. degree at Korea University, Seoul, Korea. He was awarded the Silver and Bronze Prizes respectively in the 2011 Samsung Humantech Paper Contest in February 2012. His research topics include communication theory and signal processing

techniques for multi-user MIMO wireless networks and distributed antenna systems. He is currently interested in convex optimization, random matrix theory and stochastic geometry.



Sung-Hyun Moon (S'05-M'12) received the B.S., M.S., and Ph.D. degrees in electrical engineering from Korea University, Seoul, Korea, in 2005, 2007, and 2012, respectively. Since 2012, he has been with the Electronics and Telecommunications Research Institute (ETRI), Daejeon, Korea, as a research engineer. During spring 2009, he visited the University of Southern California (USC), Los Angeles, CA, as a visiting student to conduct collaborative research under the Brain Korea 21 (BK21) Program. His current research interests include multiuser information theory and signal processing techniques for MIMO wireless cellular networks.



Inkyu Lee (S'92-M'95-SM'01) received the B.S. degree (Hon.) in control and instrumentation engineering from Seoul National University, Seoul, Korea, in 1990, and the M.S. and Ph.D. degrees in electrical engineering from Stanford University, Stanford, CA, in 1992 and 1995, respectively. From 1995 to 2001, he was a Member of Technical Staff at Bell Laboratories, Lucent Technologies, where he conducted research on high-speed wireless system designs. He later worked for Agere Systems (formerly Microelectronics Group of Lucent Technologies), Murray Hill, NJ, as a Distinguished Member of Technical Staff from 2001 to 2002. In September 2002, he joined the faculty of Korea University, Seoul, Korea, where he is currently a Professor in the School of Electrical Engineering. During 2009, he visited University of Southern California, LA, USA, as a visiting Professor. He has published around 80 journal papers in IEEE, and has 30 U.S. patents granted or pending. His research interests include digital communications and signal processing techniques applied for next generation wireless systems. Dr. Lee currently serves as an Associate Editor for IEEE TRANSACTIONS ON COMMUNICATIONS and the IEEE TRANSACTIONS ON WIRELESS COMMUNICATIONS. Also, he has been a Chief Guest Editor for the IEEE JOURNAL ON SELECTED AREAS IN COMMUNICATIONS (Special Issue on 4G Wireless Systems). He received the IT Young Engineer Award as the IEEE/IEEK joint award in 2006, and received the Best Paper Award at APCC in 2006 and IEEE VTC in 2009. Also he was a recipient of the Hae-Dong Best Research Award of the Korea Information and Communications Society (KICS) in 2011.